# ECE 445: Senior Design

Continuous Arteriovenous Fistula (AVF) Monitoring Device


Team 45

Members: Aryan Parikh, Rishab Veldur, Satyansh Yeluri

TA: Surya Vasanth



Date: 26 April, 2024

## Abstract

This paper explains the concept, design process, and results of the continuous fistula monitoring device, pitched by Richard Longfei, which aims to achieve the ability to save fistulas before they fail. This paper will begin with an overview of the problem the device aims to solve, followed by the design choices and changes made throughout the semester, and ending with the testing, challenges, and accomplishments of the device in tandem with the development board. Overall, this fistula monitoring device was accomplished through the CNN and application, and limited functionality was demonstrated through the PCB.

# 1. Introduction

## 1.1 Problem

Arteriovenous Fistulas/Grafts (AVFs/AVGs) are crucial to patients with end-stage kidney disease. They allow for hemodialysis, which has significant mortality and quality of life benefits in younger patients. Between 2000 and 2020, the prevalent count of individuals receiving HD nearly doubled to $480,516. In older patients, it's often considered a lifeline. However, AVFs are known to "go down". They are susceptible to stenosis, thrombosis, and enlargement over time, leading to high-output cardiac failure. Currently, there is no format for continuous monitoring of these grafts, and when they thrombose in the acute setting, often go undetected for days, if not weeks. The cost range to create an AV fistula is also between $3,401-$5,189. Several studies have pointed out that early graft intervention can improve the salvage of these fistulas, prolonging their use and minimizing the number of additional surgeries required. Finally, studies have found that if grafts are not intervened within 7 days, there are significant long-term mortality risks and poor patient outcomes [1].

The basic tenet for vascular access monitoring and surveillance is that stenosis develops over variable intervals in the great majority of vascular accesses and, if detected and corrected, under dialysis can be minimized or avoided (dialysis dose protection) and the rate of thrombosis can be reduced [2].

**Problem Statement: Graft stenosis and thrombosis are the leading causes of loss of vascular access patency, with delay in treatment leading to loss of vascular access increased mortality rates, and decreased quality of life in patients with end-stage renal disease.**

## 1.2 Solution

AVFs are often embedded in the arm, where the radial artery and adjacent veins are involved in their creation. What clinicians use to determine fistula viability is palpation, where the palpable trill (or vibration) of the graft can be felt. In the context of vascular access for hemodialysis, a trill is often associated with the feeling of blood flow or the movement of blood through the graft. A strong, palpable trill suggests good blood flow through the access site, indicating that the fistula is functioning well.

The idea is to develop a device that can be attached as a patch adjacent to the fistula to sample this venous trill using auditory input and machine learning to gauge deviations from an initial baseline. The device would be placed initially and cross-referenced with the current gold standard of duplex ultrasound to establish a baseline. As the device lives with the patient, it will learn progressive changes in venous hum pattern (stenosis) that can provide information to clinicians on optimal follow-up. Otherwise, if it detects the absence of a hum (thrombosis) it will immediately alert the patient and provider for attention. The pitch should correspond with an increase in the percentage of stenosis and be interpreted as more frequent oscillations in a pressure waveform over time.

**Attachment Method:** The device can be attached securely to the patient's skin using medical-grade adhesive, ensuring stability and comfort during wear.

**Proximity to the AV Fistula:** The device should be positioned in close proximity to the AV fistula to capture the venous trill accurately. It will be placed directly over the area where the fistula is created because this is the best spot for detecting the blood flow patterns.

## 1.3 Visual Aid

The image below shows a very general description of how the Arteriovenous Fistula monitoring device is placed and used. The device is placed on top of the connection of the artery and vein. The microphone records the blood pumping through the fistula and transmits and audio sample to a connected mobile device. The device is processed on the cloud and the user is able to see any changes to the condition of their fistula.

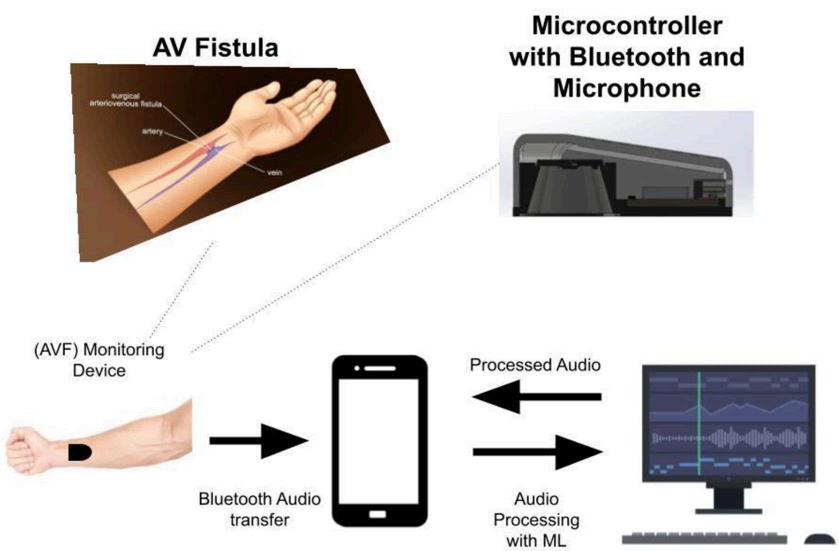


**Figure 1: Arteriovenous Fistula Monitoring Device General Design**

## 1.4 High-Level Requirements

1. The device should transmit audio signals with a minimum sampling rate of 44.1 kHz to the accompanying mobile application.
2. The device can distinguish changes in fistula stenosis (pulsatile vs continuous) correctly 75% of the time. These changes should be detected within a day, allowing for prompt intervention by healthcare providers

3. Have maximum dimensions of 3” by 2” by 2” so it is compact enough to be able to be placed on the forearm.

## 1.5 Subsystem Overview

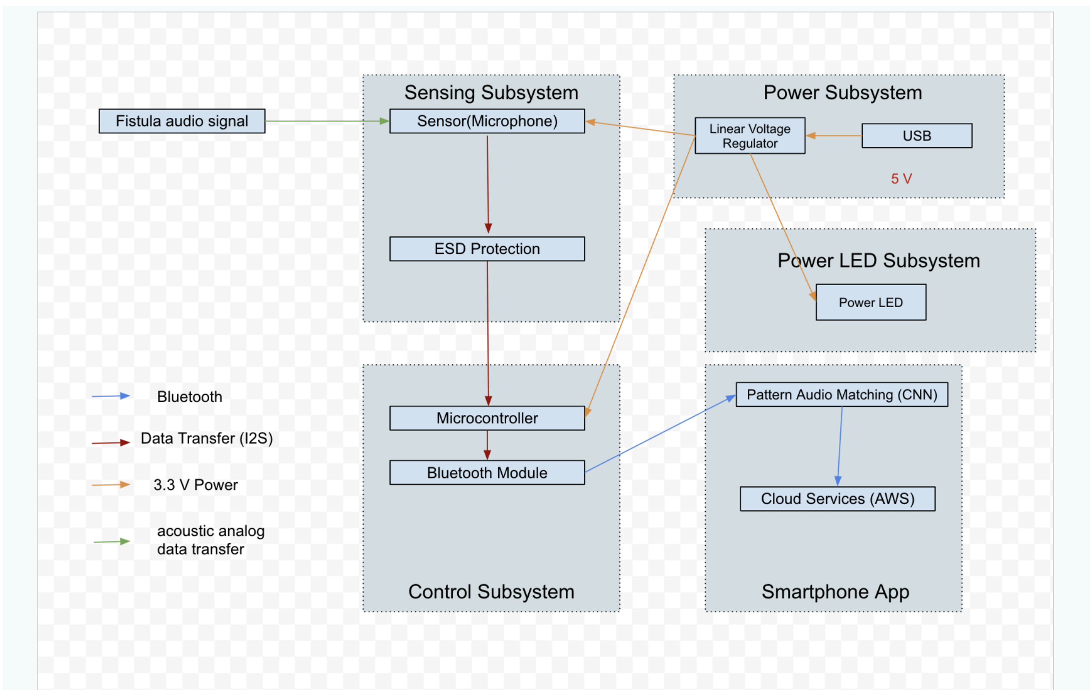


**Figure 2: Block Diagram**

Our Project has five critical subsystems: Sensing, Power, Control, Power LED, and Smartphone Application.The Sensing subsystem includes the MEMS microphone to record audio and an Electromagnetic interference filter to protect against electrostatic discharge introduced from the analog signals from the microphone. The power subsystem supplies power to the rest of the board through a linear voltage regulator. The control subsystem contains our microcontroller and uses the bluetooth module to connect and transmit recorded analog audio signals to our application. The smartphone app processes audio through a CNN hosted on the cloud and displays processed data to the user.

The sensing subsystem incorporates the SPH0641LU4H-1 microphone positioned adjacent to the AV fistula for capturing acoustic signals related to venous hum patterns. The microphone output is passed through the PRTR5V0U2X ESD protection component that helps safeguard against electrostatic discharge. Analog signal transmission makes data transfer possible to the control subsystem for frequency spectrum analysis.
The microphone chosen also has a built in amplifier that helps ensure optimal signal strength so there is no need for a separate amplifier.

The control subsystem revolves around the NINA-B306-00B-00 microprocessor, responsible for signal analysis and processing. It interacts with the sensing subsystem through analog signal input, incorporating the USB_B_Micro for communication. The microprocessor communicates with the power subsystem, managing stable voltage supply through the TPS79333-EP voltage regulator, utilizing protocol I2S. Bluetooth capabilities enable good data transmission to the mobile application, ensuring remote monitoring.

The power subsystem, driven by the TPS79333-EP voltage regulator, ensures stable voltage supply of 3.3V to the system. It interfaces with the control subsystem, providing power through USB_B_Micro and managing fluctuations through communication protocol I2S. The voltage regulator maintains a stable output voltage with a maximum deviation of ±3%.

The power LED subsystem provides visual feedback on the system's operational status, with the LED turned on when the board is operating.

The software subsystem interfaces with the control subsystem through Bluetooth communication, receiving data and alerts. This subsystem processes audio recordings to classify them based on predefined patterns utilizing cloud computing and machine learning algorithms. In audio deep learning models, spectrograms serve as a compact, image-like representation of audio signals. The process typically involves converting raw audio data into spectrograms, augmenting this data, and then using CNNs to extract features from these images. The features are then used to classify the audio as a healthy fistula or one that has closed.

# 2. Design

## 2.1 Physical Design

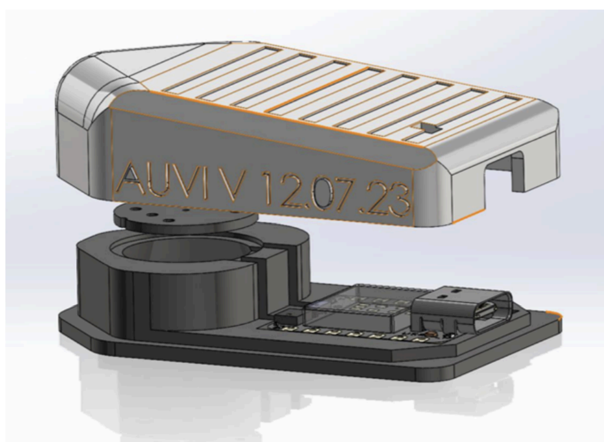


**Figure 3: Exploded view of the AUVI Device**

Designed as a patch, it consists of a PCB with bluetooth, microcontroller, and a charging element.

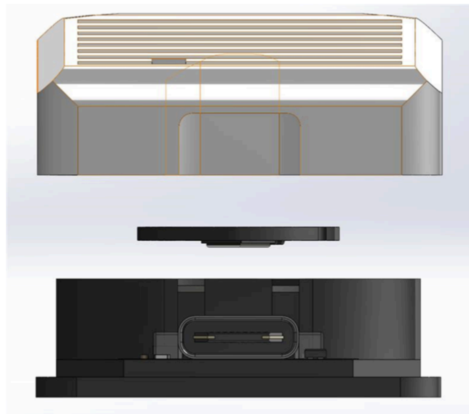

**Figure 4: Posterior view of the device, highlighting the USB port and microphone module**

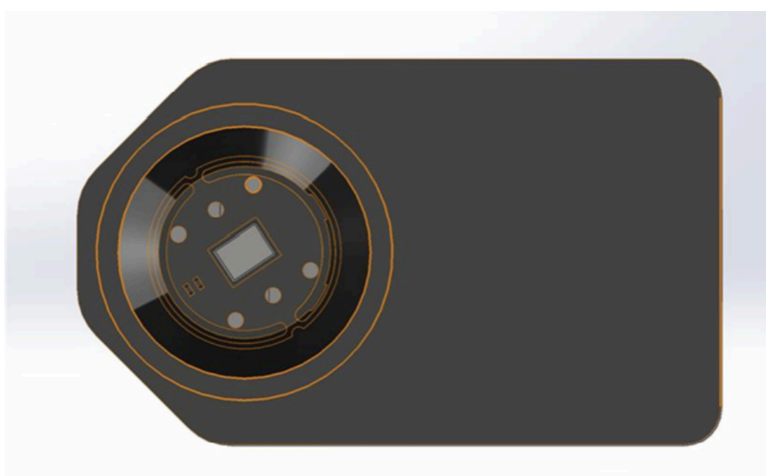

**Figure 5: Bottom view of the device.**

The bottom of the device is designed to stick to an adhesive, and the highlighted area is designed to channel signal off of the skin to the omnidirectional microphone module.

## 2.2 Equations and Simulations

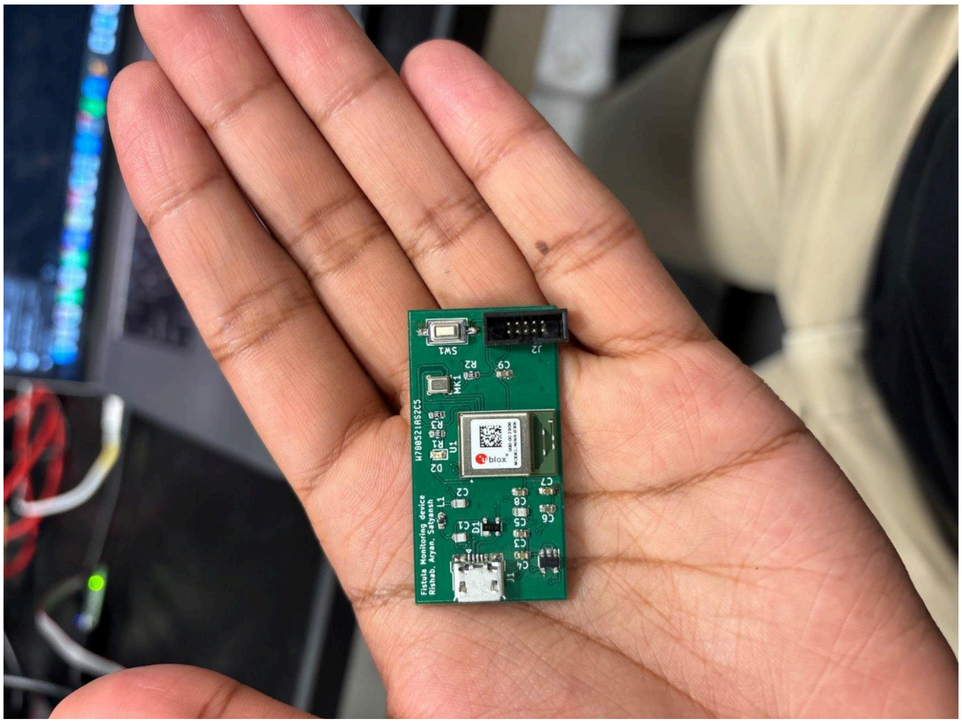

**Figure 6: PCB Design**

Estimating Model Accuracy Confidence Interval with Bootstrapping

Bootstrapping is a statistical technique that can help estimate the distribution of a statistic (like model accuracy) from the data itself, without needing to assume a normal distribution. This method can be particularly useful for understanding the variability in model performance due to the dataset's size and composition. We will use this to estimate the confidence interval for the machine learning model's accuracy, giving us insight into the reliability and tolerance of the software subsystem's performance.

Model Accuracy

From the original dataset of size N, we will randomly sample N instances with replacement to create a bootstrap sample. This sample will likely contain some duplicates and miss some instances from the original dataset.

We will train our model on this bootstrap sample and then test it on the original dataset to calculate the accuracy.

We will repeat process B = 1000 times to generate a distribution of accuracy scores.

Calculate the Confidence Interval:

From the bootstrapped distribution of accuracy scores, we calculate the desired confidence interval (e.g., the 95% confidence interval) to understand the range in which the true model accuracy is likely to fall.

Mathematical Example:

To calculate the 95% confidence interval:

We sort the bootstrapped accuracy scores in ascending order.

We find the 2.5th percentile and the 97.5th percentile values in the sorted list. These values define the bounds of the 95% confidence interval.

For example, if after sorting our accuracy scores, the 2.5th percentile value is 78% and the 97.5th percentile value is 82%, our 95% confidence interval for model accuracy is [78%, 82%].

This confidence interval provides a quantitative measure of how much the model's accuracy might vary due to variability in our dataset. A narrower interval indicates more reliable model performance, while a wider interval suggests greater sensitivity to data variability.

The TPS79333-EP voltage regulator is specified to have an output voltage of 3.3V.

The datasheet indicates that the output voltage tolerance is typically ±2%, with a maximum of ±3%.

$$Nominal\ output\ voltage\ (V\_nom)\ =\ 3.3V$$

**Typical Tolerance Range:**

**The typical output voltage tolerance is ±2% of 3.3V:**

Lower tolerance limit: V_min_usual  = 3.3V - (0.02 * 3.3V) = 3.234V

Upper tolerance limit: V_max_usual = 3.3V + (0.02 * 3.3V) = 3.366V

**Maximum Tolerance Range:**

**The maximum output voltage tolerance is ±3% of 3.3V:**

Lower tolerance limit: V_min_max = 3.3V - (0.03 * 3.3V) = 3.201V

Upper tolerance limit: V_max_max = 3.3V + (0.03 * 3.3V) = 3.399V

**Feasibility Assessment:**

We then have to make sure to check whether the tolerance ranges provided by the TPS79333-EP voltage regulator meet the system's requirements.

**Typical Tolerance Range:**

The typical output voltage tolerance ranges from 3.234V to 3.366V, which is within the acceptable range of 3.3V ± 2%. This range should be able to power the system components without exceeding their voltage ratings.

**Maximum Tolerance Range:**

The maximum output voltage tolerance ranges from 3.201V to 3.399V, which is within the acceptable range of 3.3V ± 3%. This is slightly wider than the typical range, but it still ensures that the output voltage remains within safe limits for the system.

**Conclusion:**

After doing the tolerance analysis using the specifications provided for the TPS79333-EP voltage regulator, we conclude that both the typical and maximum tolerance ranges for the output voltage appear feasible for meeting the system's requirements. The output voltage remains within acceptable limits which means that the system will have a stable power supply to the system components. Therefore, the critical subsystem function of providing stable power supply by the TPS79333-EP voltage regulator is proven feasible through our mathematical analysis.

## 2.3 Design Alternatives

Data Collection, Cleaning, and Simulation

A significant portion of our advancements in the software component is attributed to data collection, cleaning, and simulation efforts. We used a specialized fistula pump to mimic a broad spectrum of AVF flow patterns to create a dataset mirroring real-world conditions. After the design review, we made sure that this dataset has a lot of different heartbeats and we also introduced white noise so we can account for white noise that people will have in real life as well as to expand the samples.

After the design review, we also recognized the limitations of just physically collected data, so we are also going to include additional simulated data to our datasets. This simulation will replicate a wide range of venous hum patterns, encompassing both continuous and pulsatile flows. This larger dataset bolsters the training of our machine learning models, significantly enhancing their predictive accuracy and reliability. Through rigorous data cleaning, we ensure the integrity and utility of this information for our model training processes.

Machine Learning Model Development

Our technical contributions include the development and refinement of advanced machine learning models, particularly leveraging convolutional neural networks (CNNs) and recurrent neural networks (RNNs). These models undergo training on both collected and simulated data to classify the status of AVFs accurately, focusing on distinguishing between continuous vs. pulsatile flow patterns.

Convolutional Neural Networks (CNN): The development of our machine learning capabilities begins with the application of CNNs, which help identify differences between pulsatile and continuous flow patterns. The CNN's is good at analyzing visual representations of these flow patterns in the spectral data, which makes it effective at classifying the type of flow based on its characteristics.

Recurrent Neural Networks (RNN): Building upon the foundational analysis provided by the CNN, our use of RNNs takes a dynamic approach. The RNN focuses on tracking the temporal changes between pulsatile and continuous flows, analyzing the sequence of data over time to identify trends or shifts in the flow patterns. This capability is particularly valuable for predicting transitions in the fistula's condition, which will really help signal the onset of complications. By recognizing these changes early, the RNN will help our objective of preempting adverse events, offering insight that could inform timely medical intervention before the AVF fails.

Dataset Preparation: I am currently combining the synthetic signals with real-world data collected from the fistula pump simulations, ensuring a balanced and diverse dataset for training and testing.

Model Training: I am currently training the CNN model to differentiate between pulsatile and continuous flow patterns based on the spectral features of the signals. Simultaneously, training the RNN to identify temporal changes in the flow patterns that might indicate an evolving fistula condition.

Performance Evaluation: I am using a validation dataset to evaluate the models' accuracy, sensitivity, and specificity. Run simulations to test the models' response to unseen data, adjusting the architecture and parameters as necessary to improve performance.

## 2.3 Design Description and Justification

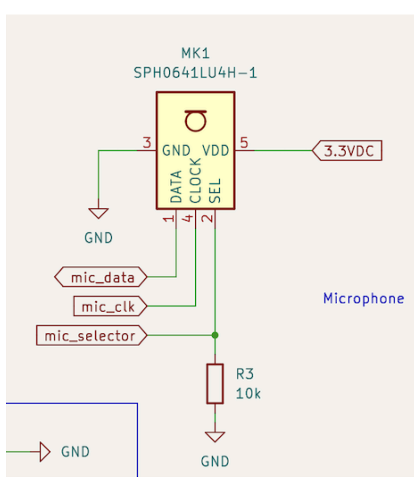

**Figure 7: Sensing Subsystem**

The selection of the SPH0641LU4H-1 microphone for our arteriovenous (AV) fistula monitoring device was driven by its superior performance characteristics, which align perfectly with our requirement to accurately capture the nuanced sounds of blood flow through the fistula. This microphone stands out for its high sensitivity and wide frequency response, making it an ideal choice for detecting the subtle, yet critical, sounds associated with the functioning of an AV fistula.

Fistula sounds typically fall within a specific frequency range, with the most critical sounds to monitor often below 1 kHz. This range includes the vital 'whooshing' sounds of blood flow that can indicate a healthy fistula, as well as any abnormal sounds that might signal a blockage or other issues. The SPH0641LU4H-1's ability to accurately capture these frequencies without significant loss ensures that the device can effectively monitor the fistula's status.

To justify the selection of this microphone, consider a signal-to-noise ratio (SNR) equation:

SNR = 20log10 (Signal Amplitude / Noise Amplitude)

Assuming the microphone effectively captures signals (fistula sounds) at an amplitude of 30 db and the background noise is at an amplitude of 20 db the SNR can be calculated. For our application, a higher SNR is critical as it indicates that the fistula sounds are much clearer relative to the background noise, allowing for more accurate monitoring and analysis.

Using the given signal amplitude of 30 dB for the fistula sounds and a background noise amplitude of 20 dB, the signal-to-noise ratio (SNR) calculation yields an SNR of approximately

3.52 dB. The SPH0641LU4H-1's performance characteristics, including its high sensitivity and ability to capture low-frequency sounds accurately, contribute to achieving a much higher SNR. This ensures that the device can reliably detect and analyze the sounds of blood flow through the fistula, making it a justified choice for our monitoring application.

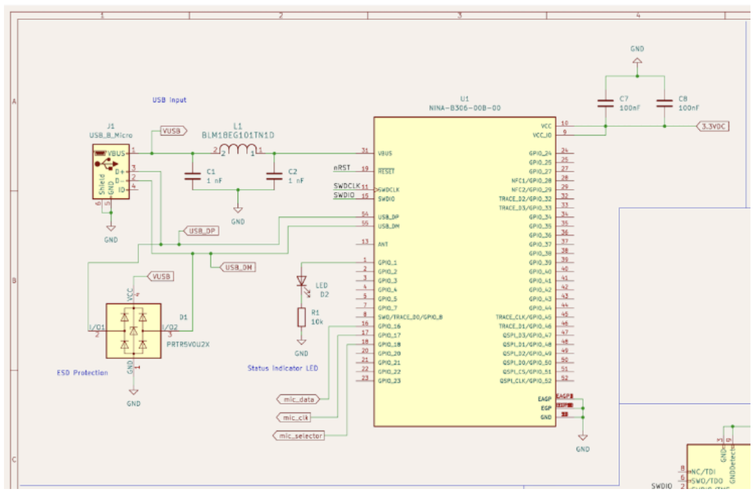


**Figure 8: Control Subsystem**

For the device's power subsystem, I integrated a microUSB port, opting for it as a direct power supply solution. The heart of this subsystem is the TPS79333-EP, a linear voltage regulator chosen for its ability to provide stable and reliable power. This steps the voltage down from 5V which is the input voltage to 3.3V which is what the parts of our board operate on. To address the challenge of high-frequency noise, which could potentially disrupt the device's sensitive readings, I engineered a noise rejection circuit. This circuit is built around a ferrite bead, the BLM18G101TN1D, known for its effectiveness in filtering high-frequency noise. Alongside this, I incorporated two 1nF capacitors in parallel, enhancing the circuit's ability to maintain a clean power supply by further smoothing out any residual electronic disturbances. This approach ensures that the device operates with optimal precision and reliability.

Incorporating an Electrostatic Discharge (ESD) protection circuit into our device was a critical step to ensure its longevity and reliability, especially in a medical setting where it will be subjected to various environmental factors that could potentially cause damage. For this purpose, we chose the PRTR5V0U2X series for ESD protection, a decision driven by its robust performance in safeguarding sensitive electronic components against the abrupt and potentially damaging effects of ESD events.:

Dual-Line Protection: The PRTR5V0U2X offers protection for two lines with a single component, making it an efficient choice for compact PCB designs where space is at a premium. This is particularly important in wearable medical devices, where minimizing size without compromising on protection is crucial.

Low Clamping Voltage: This ESD protection device has a low clamping voltage, which means it can effectively clamp down on the voltage during an ESD event to a level that is safe for the sensitive electronics in our device. This is essential for preventing damage that could lead to device failure or inaccurate readings.

High Surge Capability: The component is capable of handling significant surge currents, ensuring that even in the case of a strong ESD event, the protection circuit can absorb the excess energy without being damaged itself.

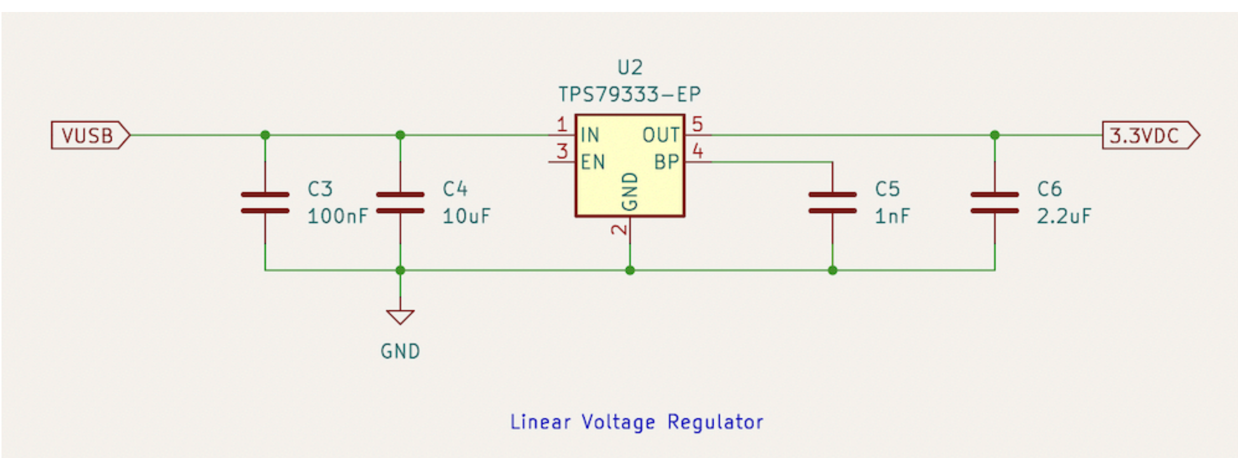

**Figure 9: Power Subsystem**

We have chosen a 5V Lithium Polymer (LiPo) battery as our primary power source. This decision was guided by several factors including the battery's rechargeability and form factor which is ideal since our device is supposed to be compact and portable.

Battery Specifications

Type: Rechargeable Lithium Polymer (LiPo) Battery

Voltage: 5V

Capacity: 2000mAh, this provides us with a good balance between longevity and the actual physical size.

The integration of the battery into our power subsystem is really important in our design. The battery connects directly to a power management module that includes safe charging and discharging. This module ensures protection against overcharging, deep discharging, and short circuits, thereby extending the battery's lifespan and maintaining user safety.

To accommodate the microcontroller and other components requiring regulated 3.3V power, a voltage regulator (model TPS79333-EP) steps down the 5V from the battery to a stable 3.3V output. This regulator was selected for its low dropout voltage and overall efficiency.

The regulated 3.3V output from the TPS79333-EP is distributed to the NINA-B306-00B-00 microcontroller and other critical subsystems, such as the sensing and control units.

Power Management: This system minimizes energy waste and maximizes battery life by providing each component with the precise voltage it requires for optimal operation. Through this method, we ensure that the device remains energy-efficient, extending the operational duration between charges while maintaining high performance and reliability.

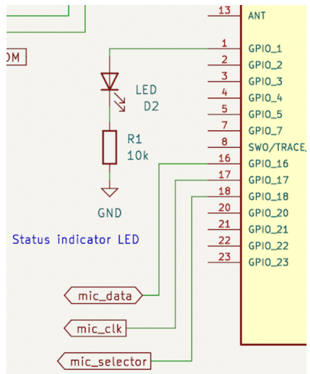


**Figure 10: Power LED Subsystem**

A status indicator LED was added to the design in order to show when the device is recording for privacy reasons as well as when the device is turned on. This provides a quick indicator that doesn't require software for debugging and patient interaction.

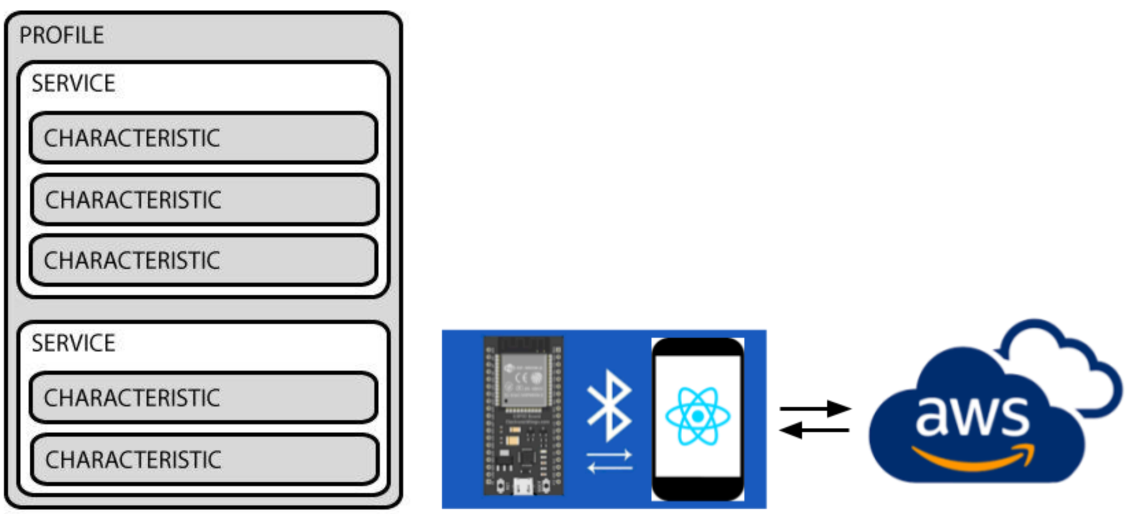


**Figure 11/12: Software Components/Bluetooth**

The technical implementation of this project required a detailed understanding of various technologies, including the microcontrollers, Bluetooth Low Energy (BLE) communication, React application development, and AWS services. Each component played a crucial role in the seamless operation of the system, from recording audio to processing it in the cloud. I initiated the development of this subsystem using a XIAO ESP32 microcontroller as a development board, equipped with Bluetooth and microphone functionalities. The following sections detail the technical nuances and interfaces between the working with the development board and the expected changes needed to make it work with our final PCB design.

Microcontroller

At the heart of the project lies a microcontroller with integrated BLE capabilities, making it an ideal candidate for IoT applications. The ESP32 was programmed to record three second audio samples at 30-minute intervals, leveraging its I2S (Inter-IC Sound) interface for high-quality audio input. The I2S protocol, known for its ability to handle stereo audio at various sample rates, was connected to an external microphone for capturing sound. The same program should work with the NINA board since the NINA board uses the I2S protocol as well to interface with a microphone.

Audio Recording and Storage

The audio recording functionality was implemented via a custom program written in C, utilizing the esp_i2s library, which provides comprehensive support for the ESP32's hardware features. The firmware was designed to initiate recording based on a timer interrupt, ensuring that audio capture occurred precisely every 30 minutes. To manage the resulting audio files, the ESP32's external SD card was used for storage. Files were stored in a compressed format to optimize space and facilitate quicker BLE transmission. For the NINA board, the same i2s library should work but the program needs to be modified to use the NINA onboard file system to save temporary recording samples [5].

## BLE Communication

At the core of Bluetooth Low Energy (BLE) communication is the Generic Attribute Profile (GATT), which structures data exchange through a hierarchical system of services, characteristics, and descriptors. Unique identification of these elements is achieved using Universally Unique Identifiers (UUIDs), which come in 128-bit or 16-bit codes, ensuring that data points are distinct across all BLE devices. Data transfer in GATT operates through read and write operations, where a central device requests or sends data to a peripheral device [6].
GATT capabilities were harnessed to create a custom BLE service for the project. This service included several characteristics, such as file size, total number of data chunks, current chunk number, and acknowledgments for received chunks. These characteristics allowed for detailed control and monitoring of the file transfer process from the microcontroller to the React application [7].

## React Application

The React application served as the BLE client, connecting to the board and managing the file transfer process. Developed using the popular JavaScript library React, the application provided a user-friendly interface for initiating connections, receiving data, and displaying processed results.

BLE Integration with react-native-ble-plx

Integration with the BLE service was achieved using the react-native-ble-plx library, a React Native package designed for cross-platform BLE communication. The library facilitated the discovery of BLE devices, connection to the ESP32, and interaction with the custom BLE service's characteristics. The application implemented logic to handle the reception of data chunks, reassemble them into the original audio file, and acknowledge the receipt of each chunk to the board, ensuring reliable data transfer [8].

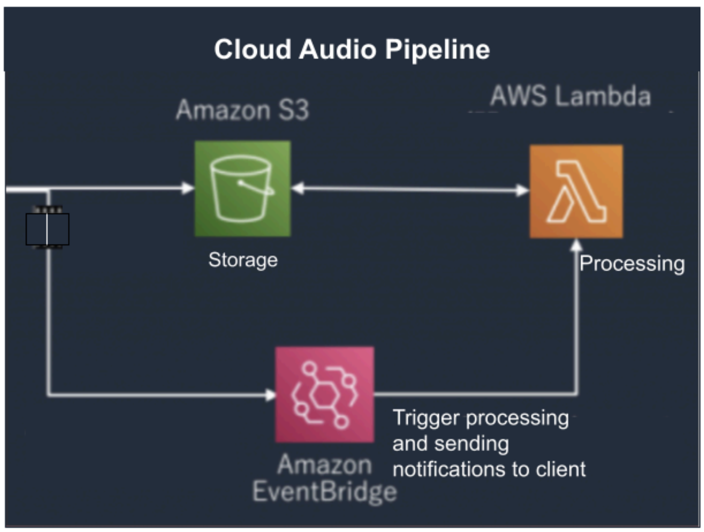


**Figure 13: Cloud Audio Pipeline**

AWS S3 and Lambda Integration

Upon successfully receiving and assembling the audio file, the React application uploaded it to AWS S3. This process utilized the AWS SDK for JavaScript, enabling secure and efficient file uploads to a designated S3 bucket. Following the upload, an AWS Lambda function was triggered to process the audio file. This serverless function was designed to clean and preprocess the data, making it suitable for analysis by a machine learning model hosted on AWS. The Lambda function utilized various AWS services, such as Amazon S3 for accessing the file and Amazon SageMaker for interfacing with the machine learning model.

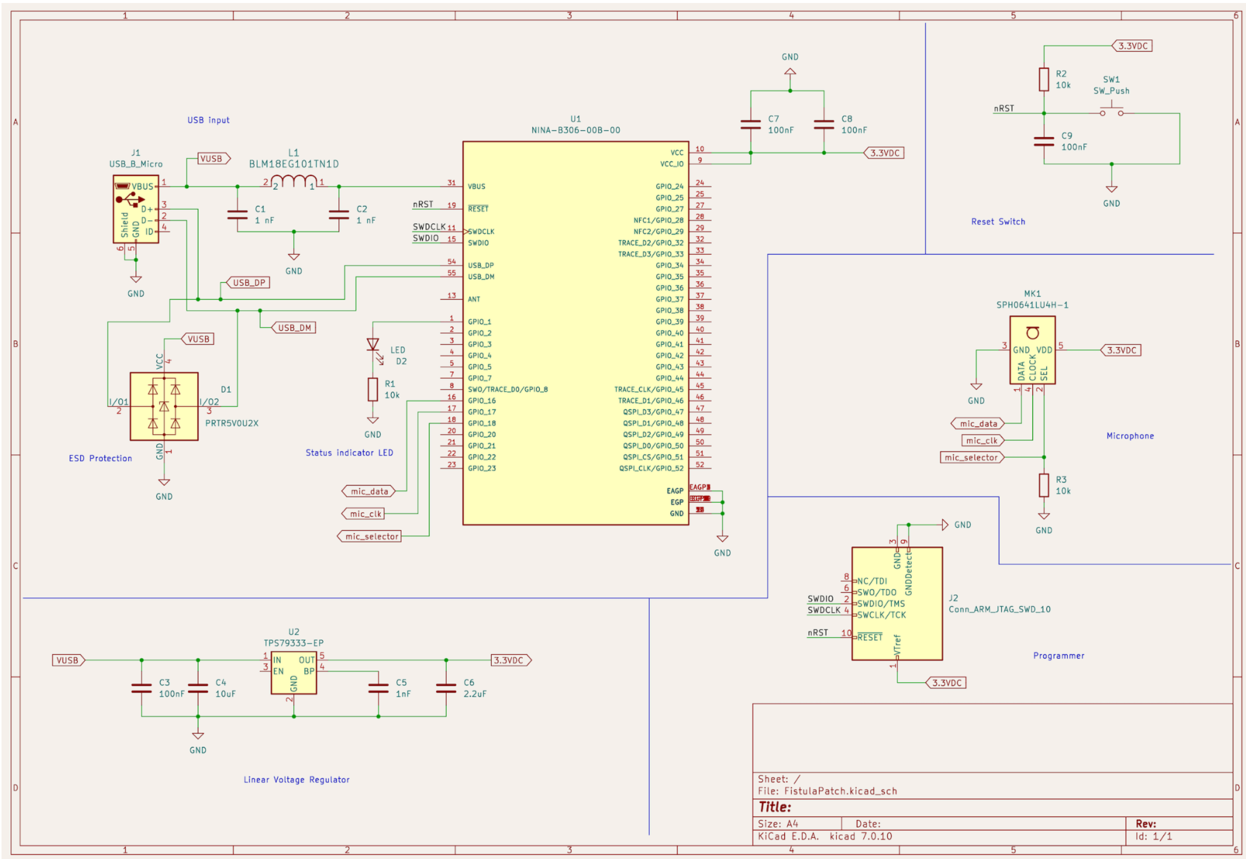


**Figure 14: Full PCB Design**

## 3. Cost Analysis

The average salary for a student graduating with an electrical engineering degree and computer engineering degree at University of Illinois Urbana-Champaign is around $104,000 [4]. For 50 work weeks at 40 hours per week, this comes out to $52/hour. The project is estimated to take 8 hours of work per week and per person. We calculated using 9 weeks as designing actually starts during week 5 of class and we have spring break in between. Therefore to complete this project, it results in 72 total hours per person (8 * 9). We will not be utilizing the machine shop for our project. We will also multiply our costs by 2.5 to account for any overhead for the development of this project. $52/hour * 2.5 * 72 = $9,360 per person * 3 = $28,080 in labor costs for the project.

| Part Expenses | | | |
|---|---|---|---|
| Part Name | Quantity | Cost | Link |
| Capacitors 1nF | 3 | $1.62 | https://www.digikey.com/en/products/detail/kemet/C0805C102K5GECAUTO/16680427?utm_adgroup=&utm_source=google&utm_medium=cpc&utm_campaign=PMax%20Supplier_Focus%20Supplier&utm_term=&utm_content=&utm_id=go_cmp-20243063242_adg-_ad-__dev-m_ext-_prd-16680427_sig-EAIaIQobChMIxPbNmsqQhQMVY9zjBx34qA55EA0YAiABEgImNvD_BwE&gad_source=1&gbraid=0AAAAADrbLli7upNbGjglEExpne-VkHlRB&gclid=EAIaIQobChMIxPbNmsqQhQMVY9zjBx34qA55EA0YAiABEgImNvD_BwE |
| Capacitors 2.2uF | 1 | $0.40 | https://www.digikey.com/en/products/detail/kemet/C0603C225K8PAC7867/1090906?utm_adgroup=&utm_source=google&utm_medium=cpc&utm_campaign=PMax%20Supplier_Focus%20Supplier&utm_term=&utm_content=&utm_id=go_cmp-20243063242_adg-_ad-__dev-m_ext-_prd-1090906_sig-EAIaIQobChMIsNeclcuQhQMV1aFaBR1WEQ7vEAQYASABEgI1gPD_BwE&gad_source=1&gbraid=0AAAAADrbLli7upNbGjglEExpne-VkHlRB&gclid=EAIaIQobChMIsNeclcuQhQMV1aFaBR1WEQ7vEAQYASABEgI1gPD_BwE |
| Capacitors 10uF | 1 | $0.60 | https://www.digikey.com/en/products/detail/murata-electronics/GRM188C80G106KE47D/5026386?utm_adgroup=&utm_source=google&utm_medium=cpc&utm_campaign=PMax%20Supplier_Focus%20Supplier&utm_term=&utm_content=&utm_id=go_cmp-20243063242_adg-_ad-__dev-m_ext-_prd-5026386_sig-EAIaIQobChMImbyn2MqQhQMVd2dHAR3_7QhYEAQYAyABEgJ2pvD_BwE&gad_source=1&gbraid=0AAAAADrbLli7upNbGjglEExpne-VkHlRB&gclid=EAIaIQobChMImbyn2MqQhQMVd2dHAR3_7QhYEAQYAyABEgJ2pvD_BwE |
| Capacitors 100nF | 4 | $2.42 | https://www.digikey.com/en/products/detail/kemet/C0603C104K3RAC7081/12701599?utm_adgroup=&utm_source=google&utm_medium=cpc&utm_campaign=PMax%20Supplier_Focus%20Supplier&utm_term=&utm_content=&utm_id=go_cmp-20243063242_adg-_ad-__dev-m_ext-_prd-12701599_sig-EAIaIQobChMI9fHZ68mQhQMV6JxaBR0K6AEWEAQYASABEgIWHvD_BwE&gad_source=1&gbraid=0AAAAADrbLli7upNbGjglEExpne-VkHlRB&gclid=EAIaIQobChMI9fHZ68mQhQMV6JxaBR0K6AEWEAQYASABEgIWHvD_BwE |

| | | | |
|---|---|---|---|
| Resistors 10k | 3 | $1.00 | https://www.digikey.com/en/products/detail/yageo/RC0603FR-1310KL/12756437?utm_adgroup=Yageo&utm_source=google&utm_medium=cpc&utm_campaign=PMax%20Shopping_Supplier_Yageo&utm_term=&utm_content=Yageo&utm_id=go_cmp-17816160916_adg-_ad-__dev-m_ext-_prd-12756437_sig-EAIaIQobChMIwsCwstCQhQMVcWBHAR3ZNwdtEAQYASABEgJGm_D_BwE&gad_source=1&gbraid=0AAAADrbLliV4j6oUcADCNqe6ov8iQorI&gclid=EAIaIQobChMIwsCwstCQhQMVcWBHAR3ZNwdtEAQYASABEgJGm_D_BwE |
| NINA-B306-00B-00 | 1 | $14.35 | https://www.digikey.com/en/products/detail/u-blox/NINA-B306-00B/10257713?utm_adgroup=&utm_source=google&utm_medium=cpc&utm_campaign=PMax%20Shopping_Product_Medium%20ROAS%20Categories&utm_term=&utm_content=&utm_id=go_cmp-20223376311_adg-_ad-__dev-c_ext-_prd-10257713_sig-Cj0KCQjw8J6wBhDXARIsAPo7QA_HfXsuiNnml8WKj-3ORaxi-v_tj0cBJ_R5Pqy8YFllmMmVTicJHyAaAhlXEALw_wcB&gad_source=1&gclid=Cj0KCQjw8J6wBhDXARIsAPo7QA_HfXsuiNnml8WKj-3ORaxi-v_tj0cBJ_R5Pqy8YFllmMmVTicJHyAaAhlXEALw_wcB |
| USB_B_Micro | 1 | $1.95 | https://www.mouser.com/ProductDetail/Amphenol-FCI/10103594-0001LF?qs=EnLMdcWnKABYZwdMsmC%2Fag%3D%3D&mgh=1&utm_id=17222215321&gad_source=1&gclid=EAIaIQobChMI3KrkgMyQhQMVh3BHAR2R-AVgEAQYAyABEgIvCvD_BwE |
| PRTR5V0U2X ESD | 1 | $0.420 | https://www.mouser.com/ProductDetail/Nexperia/PRTR5V0U2X215?qs=LOCUfHb8d9sDkqY4cRj8Lw%3D%3D |
| SPH0641LU4H-1 | 1 | $2.14 | https://www.digikey.com/en/products/detail/knowles/SPH0641LU4H-1/5332438 |
| BLM18EG101TN1D Inductor | 1 | $0.21 | https://www.mouser.com/ProductDetail/Murata-Electronics/BLM18EG101TN1D?qs=rjbY5pkpCp4yQ17nVbKqBw%3D%3D |
| LED | 1 | $0.15 | https://www.digikey.com/en/products/detail/würth-elektronik/150060AS75000/10468330?utm_adgroup=&utm_source=google&utm_medium=cpc&utm_campaign=PMax%20Supplier_Focus%20Supplier&utm_term=&utm_content=&utm_id=go_cmp-20243063242_adg-_ad-__dev-m_ext-_prd-10468330_sig-EAIaIQobChMIkMOw2suQhQMVBtXjBx2gsAo_EAQYASABEgLibPD_BwE&gad_source=1&gbraid=0AAAAADrbLli7upNbGjglEExpne-VkHIRB&gclid=EAIaIQobChMIkMOw2suQhQMVBtXjBx2gsAo_EAQYASABEgLibPD_BwE |

| | | | |
|---|---|---|---|
| Conn_ARM_JTAG_SWD_10 | | $1.50 | https://www.digikey.com/en/products/detail/molex/0702461004/2405283?utm_adgroup=&utm_source=google&utm_medium=cpc&utm_campaign=PMax%20Supplier_Focus%20Supplier&utm_term=&utm_content=&utm_id=go_cmp-20243063242_adg-_ad-__dev-c_ext-_prd-2405283_sig-CjwKCAjw5ImwBhBtEiwAFHDZx5tBPYqGu7J2V6av4Yie5m29PvtMirxkHB8RksBNLRFeBSb29_wzTxoCIUEQAvD_BwE&gad_source=1&gclid=CjwKCAjw5ImwBhBtEiwAFHDZx5tBPYqGu7J2V6av4Yie5m29PvtMirxkHB8RksBNLRFeBSb29_wzTxoCIUEQAvD_BwE |

$26.19 + $28,080 = $28,106.19

The total cost for the project is the Labor Cost for all three members and the parts total is $28,106.19

## 4. Schedule

| Week | Task | Person Assigned |
|---|---|---|
| February 26 - March 1 | Finish working on PCB design | Rishab |
| | Start basic outline of the app | Satyansh<br>Aryan |
| March 4 - March 8 | Review PCB design | Rishab |
| | PCB Design Feedback and Assemble PCB Board | All |
| March 18 - March 22 | Start getting audio samples | All |
| | Continue working on app | Satyansh |

| | | |
|---|---|---|
| | | Aryan |
| March 25 - March 29 | Teamwork Evaluation 1 | All |
| | PCB Design Feedback and Assemble PCB Board | Rishab<br>Aryan |
| | Continue working on app | Satyansh |
| April 1 - April 5 | Assemble PCB Board | All |
| | Final additions to application | All |
| April 8 - April 13 | Test PCB Design and functionality | Rishab |
| | Work on increasing accuracy of Machine Learning algorithm | Satyansh<br>Aryan |
| | Finish creating app | All |
| April 15 - April 19 | Mock demo + fix issues | All |
| April 22 - April 26 | Final Demo<br>Work on Presentation | All |
| April 29 - May 3 | Final presentation | All |

## 5. Requirements and Verification

| Requirement | Verification | Results |
|---|---|---|
| Test whether the microphone is detecting abnormalities in fistula sounds. | Test the microphone's output by feeding it into the machine learning algorithm. Use known good and bad fistula sound samples to ensure the system accurately identifies each. | The microphone is detecting abnormalities in fistula sounds as the SVM/CNN Precision, Recall, and F1-scores all increased drastically as shown in the figure 16. |
| To assess the fidelity of audio recordings captured by the ESP32. | The recordings were analyzed for clarity, noise levels, and fidelity using audio analysis software. | Recordings had a signal-to-noise ratio (SNR) of 30 dB, with minimal distortion. |
| measure the output voltage of the TPS79333-EP linear voltage regulator to ensure it matches the expected output (3.3V) | Use a multimeter to verify that the voltage is stable and within the tolerances required for the device's operation (+- 5% | We verified that the voltage is stable by using the multimeter |
| Noise Rejection Circuit Evaluation | Use an oscilloscope to measure the noise on the power lines before and after the noise rejection circuit. | Saw a significant reduction in high-frequency noise after the noise rejection components. |
| Power LED is for visual feedback. It is used just to let us know that the system is functioning. | The power LED turns on when the board is operational. | The power LED did turn on when the board was operational |
| Get additional samples of data for continuous and pulsatile flow to improve the accuracy of the machine learning algorithms | Change the heartbeat rate to receive additional samples Add white noise and get more samples | We were able to change the heartbeat rate and get an abundant number of samples. We also added white noise as a patient will be wearing this |

| | | |
|---|---|---|
| | Take 1 minute samples and use samples between different intervals such as 1-3 seconds, 4-7 seconds. | throughout the day making sure that sound anomalies are accounted for. |
| We needed more fake samples of data for continuous and pulsatile flow as the quality of the training data directly impacts the accuracy and reliability. | We created an algorithm that gave us around 15000 different data points to distinguish between pulsatile and continuous flow. | The increase in samples helped increase the accuracy and reliability of the CNN as shown through the Precision, Recall, and F1-score.<br>(figure 16) |
| The development of our machine learning capabilities begins with the application of CNNs, which help identify differences between pulsatile and continuous flow patterns. | The CNN machine learning algorithm has an accuracy rate of at least 75%. | CNN machine learning algorithm had an accuracy over 75% (figure 16) |
| The device must be situated in an enclosure that is at most 3x2.x2 in dimension. | Measure all sides of the enclosure using a tape measure | The size of the device was well below 3x2x2 in dimension. |
| To verify the BLE connection stability between the PCB (peripheral) and the central device. | The PCB was programmed to advertise its presence continuously. The central device, a smartphone running a BLE scanner app, attempted to connect to the PCB. Upon connection, a simple data packet was sent back and forth every second for a duration of 10 minutes. | The connection was established within 3 seconds 100% of the time across 10 trials. No disconnections were observed, and all packets were successfully exchanged, demonstrating stable BLE connectivity. |

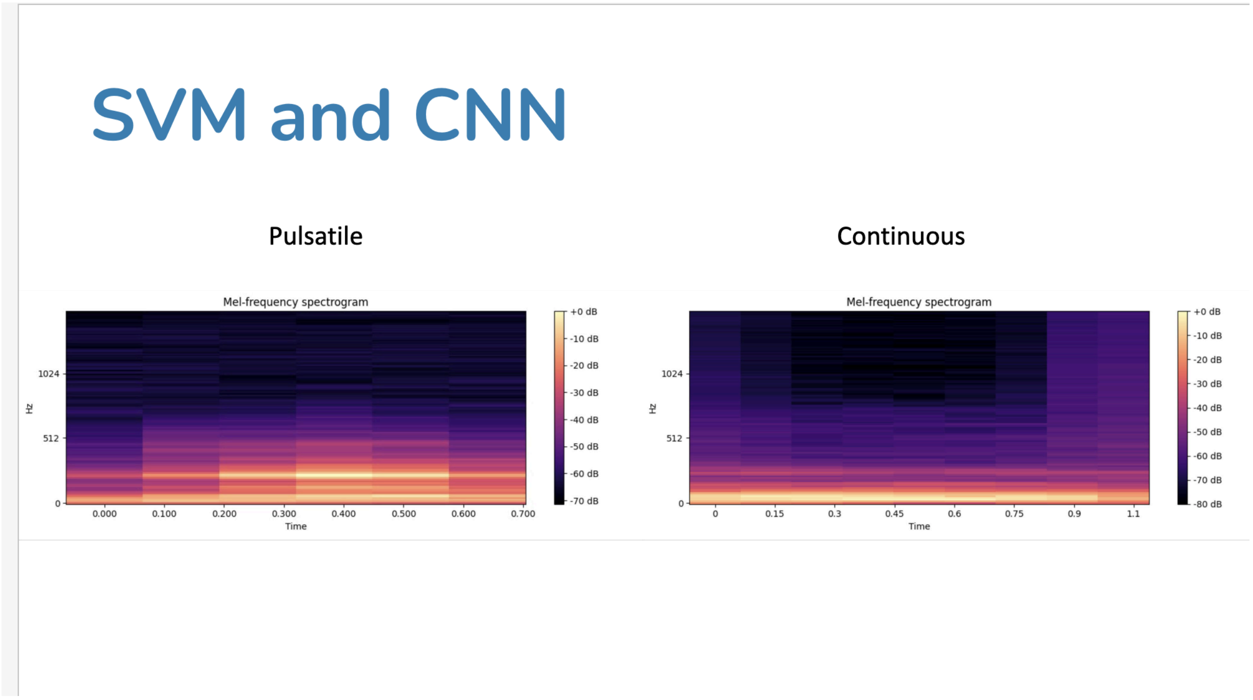


**Figure 15: Pulsatile and Continuous flow spectrogram**

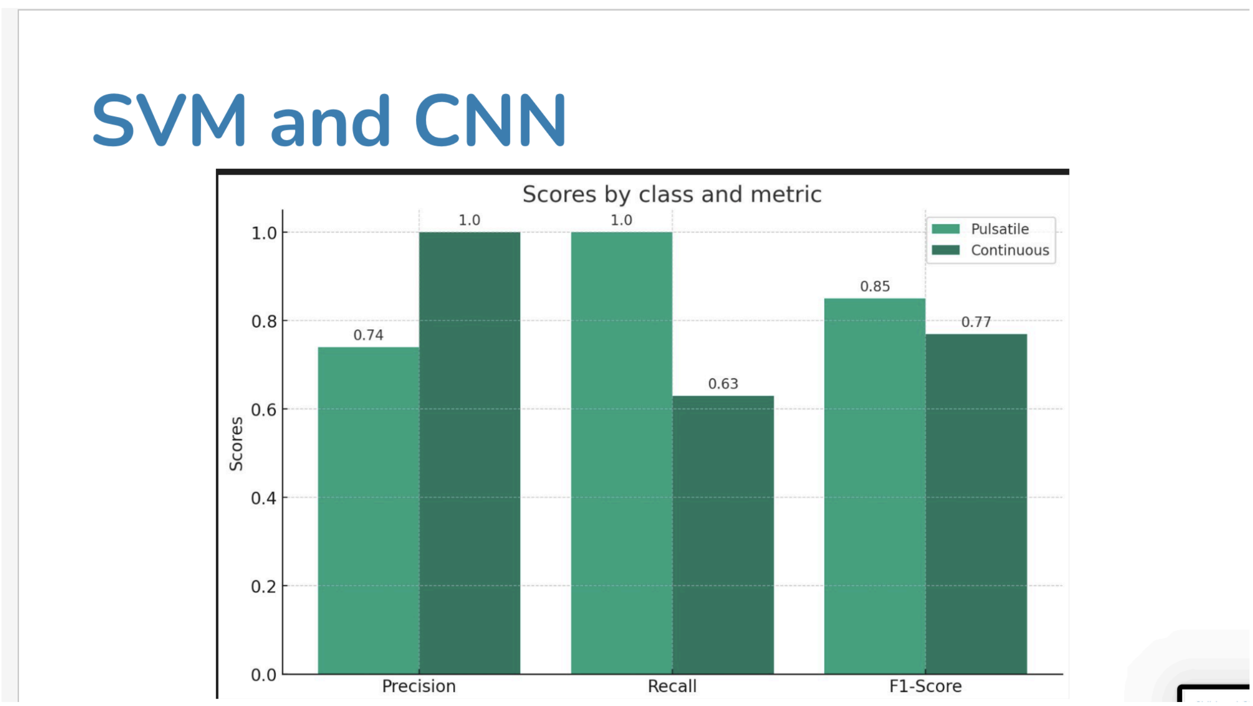

**Figure 16: SVM and CNN results**

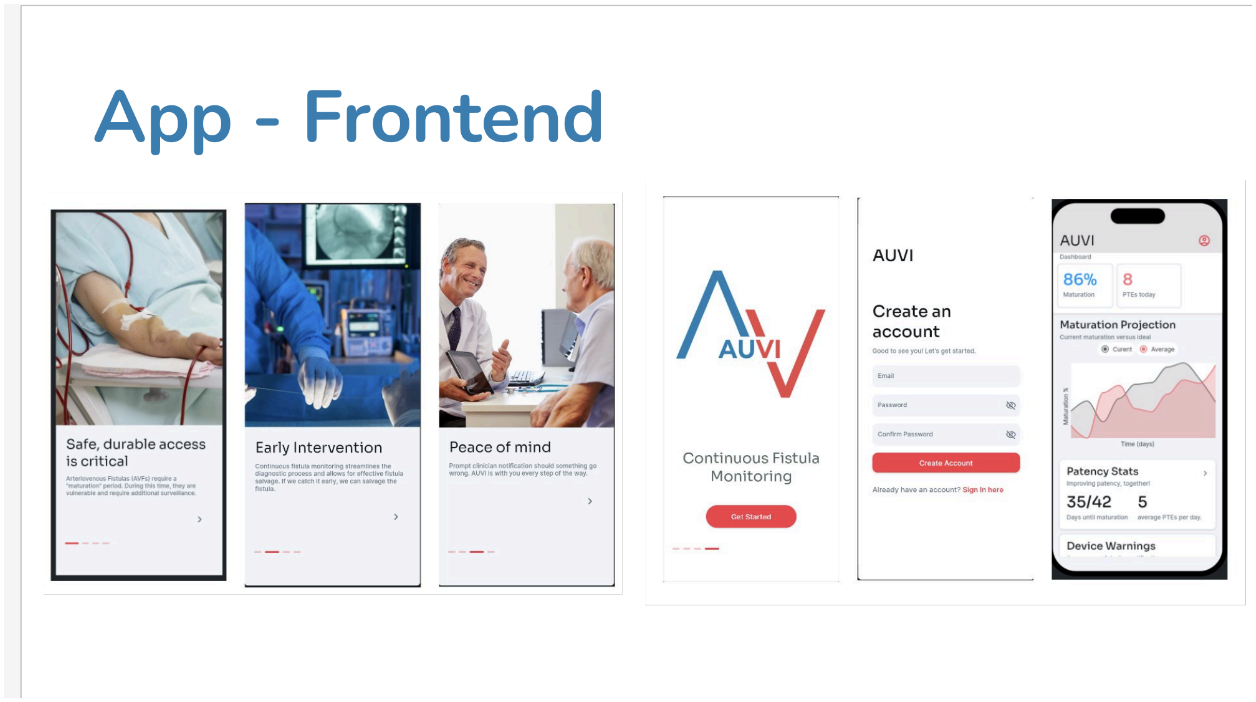


**Figure 17: App UI**

## 6. Conclusion

Accomplishments

Looking back on the progression of this project, we are proud of the successes we were able to achieve. Given that we designed our PCB with PCBWay full turnkey assembly in mind, the fact that we were able to hand-solder components onto our board was a feat in and of itself. We are glad that our PCB was able to get recognized by the computer and enumerate as this confirmed the microcontroller was correctly soldered to the PCB, turned on, and ran a program. Finally, we are proud that we were able to replicate fake sounds for both pulsatile and continuous as gathering thousands of samples was tough. We took Professor Gruev's advice and actually created a CNN that outputted great accuracy and reliability. This experience revealed to us that continuous fistula monitoring is possible and could even turn into a start-up.

Uncertainties

The main reason why we cannot test our RNN yet is because we haven't figured out a way to differentiate times when flow is not continuous or pulsatile. We need to figure out how to change the simulated human fistula pump so that our continuous fistula monitoring device can predict when the fistula is going to go bad, instead of just when it has already failed. We also just recorded our first samples with the PCB accurately after the demo date as we found a MEMS microphone that could collect high frequency sounds. Now we also need to work on cutting the size of our PCB by half because patients will be wearing this device continuously for a long period of time.

Precision scores were also really biased towards pulsatile at 1.0 vs 0.74 for continuous. We believe this is due to the fact that the sound for continuous is so quiet that the results are biased towards pulsatile when there is white noise added. This is also something we will have to look deeper into as we don't want our machine learning algorithm facing bias.

Future Work

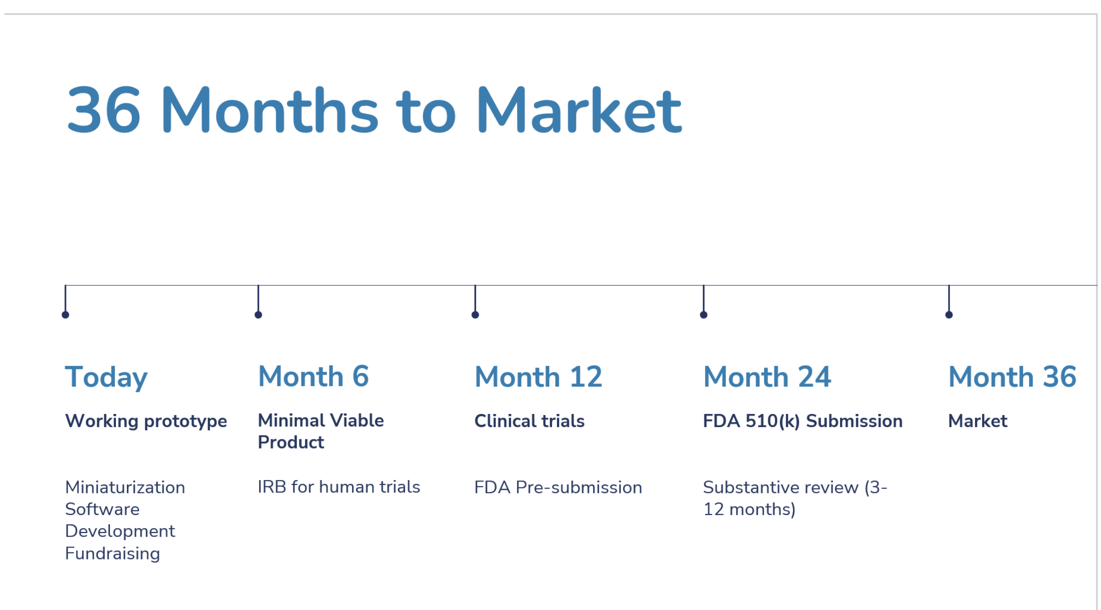

## 7. Ethics

During development, ensuring the reliability and safety of the project is very important to prevent complications in medical procedures such as misdiagnosis or incorrect incisions, which could jeopardize patient health and safety. To mitigate these risks, a comprehensive review of the project and technical quality will be conducted before any potential clinical usage. We will make sure that areas where the development team lacks expertise will be supplemented with consultation from appropriate specialists by those who pitched us this project.

Safety and Regulatory Standards Industry Standards: Within the medical device industry, regulations will be determined by the intended use case of the technology. For instance, if the desire is to use it as a preliminary tool for a patient diagnosis of skin cancer, it could potentially qualify as a Class II device and follow the FDA's guidelines for further development in a clinical setting.

Accidental misuse of the product due to a lack of understanding of its limitations in a clinical setting is a significant concern for patient safety. Therefore, it is very important to standardize aspects such as the device's durability and its appropriate usage in patient settings to prevent potential complications. Additionally, thorough testing of the device's diagnostic capabilities is essential to ensure accurate diagnoses and prevent patient misdiagnosis [4].

For the software component of this project, particularly when dealing with audio recordings that might contain sensitive health-related information, adhering to ethical considerations and the Health Insurance Portability and Accountability Act (HIPAA) is crucial. Ensuring the protection and confidentiality of any health information that may be captured or processed is paramount, given the potential for recordings to include identifiable health information.

To uphold the highest ethical standards and ensure compliance with HIPAA, this project leverages cloud platforms known for their HIPAA compliance, with a specific focus on Amazon Web Services (AWS). AWS is HIPAA-certified, offering a secure environment that meets the stringent requirements necessary for handling sensitive patient data. This includes implementing robust safeguards such as end-to-end encryption for data both in transit and at rest, stringent access controls, and regular security assessments to mitigate any potential vulnerabilities.

## 8. References

[1] Grainger Engineering Office of Marketing and Communications. (n.d.). *Salary averages*. Electrical & Computer Engineering | UIUC. https://ece.illinois.edu/admissions/why-ece/salary-averages

[2] Home Page: American Journal of Kidney Diseases. (n.d.). https://www.ajkd.org/article/S0272-6386(11)00070-9/fulltext

[3] U.S. Department of Health and Human Services. (n.d.). *Annual data report*. National Institute of Diabetes and Digestive and Kidney Diseases. https://usrds-adr.niddk.nih.gov/2022/end-stage-renal-disease/1-incidence-prevalence-patient-characteristics-and-treatment-modalities

[4] IEEE code of Ethics. IEEE. (n.d.). https://www.ieee.org/about/corporate/governance/p7-8.html

[5] Bluetooth for both versions: Seeed Studio Wiki. Seeed Studio Wiki RSS. (n.d.). https://wiki.seeedstudio.com/xiao_esp32s3_bluetooth/#ble-serverclient

[6] Esp32 bluetooth getting started: ESP32. ElectronicWings. (n.d.). https://www.electronicwings.com/esp32/esp32-bluetooth-getting-started

[7] Microphone usage for sense version: Seeed studio wiki. Seeed Studio Wiki RSS. (n.d.-b). https://wiki.seeedstudio.com/xiao_esp32s3_sense_mic/

[8] Nkolban. (n.d.). ESP32_BLE_Arduino . GitHub. https://github.com/nkolban/ESP32_BLE_Arduino/tree/adc2aee2f0d01eb6b30dd5ad3589f2cc89934beb

[9] React-native-ble-PLX 3.1.2: Documentation. react-native-ble-plx 3.1.2 | Documentation. (n.d.). https://dotintent.github.io/react-native-ble-plx/#blemanager